SUPPLEMENTAL MATERIAL

IL-13-induced airway mucus production is attenuated by MAPK13 inhibition

Yael Alevy, Anand C. Patel, Arthur G. Romero, Dhara A. Patel, Jennifer Tucker, William T. Roswit, Chantel A. Miller, Richard F. Heier, Derek E. Byers, Tom J. Brett, and Michael J. Holtzman

Supplemental Methods

Primary-culture human airway epithelial cells. Human tracheal epithelial cell (hTEC) cultures were seeded at 2 x 10^4 cells per well (24-well Transwell, Corning, Corning, NY) and cultured under submerged conditions until confluent. Cultures were then maintained in DMEM-Ham's F12 medium with 2% NuSerum (BD, Franklin, NJ), Primocin (100 µg/ml, InvivoGen, San Diego, CA), and retinoic acid (1 x 10^{-8} M, Sigma) with or without IL-13 (50 ng/ml, Peprotech, Rocky Hill, NJ).

Chemical inhibitors. BIRB-796 (Doramapimod) was obtained from American Custom Chemicals (San Diego CA). SB-203580 was obtained from EMD Chemicals (Gibbstown, NJ). These compounds and all analogs were also synthesized in our laboratories and purified to >99% purity using silica gel column chromatography and recrystallization. Purity analysis was determined using a Zorbax XDB-C8 column on an Agilent Series 1100 LC-MS instrument with UV detection at 215 and 254 nM. ^{1}H NMR spectra were obtained using a Varian 400 MHz NMR instrument. Instant JChem (version 5.9.3, 2012 release) was used for structure database management and search (http://www.chemaxon.com). Compounds were stored in the dark at 10 mM in DMSO before use in biological or biochemical assays.

Gene expression microarray analysis. Gene expression analysis was performed using Illumina Human HT-12 BeadChip (Illumina, San Diego, CA, USA). Total RNA was isolated from hTECs using the Qiagen RNEasy kit (Qiagen) and was amplified and biotinylated using the Ambion Illumina TotalPrep Kit. Hybridization and scanning, including background correction, of Human HT-12 BeadChip arrays was performed according to the manufacturer's instructions, using BeadStudio 3.0 software (Illumina) at the Washington University School of Medicine Genome Sequencing Center Microarray Core Facility. Microarray normalization and statistical analysis was performed using packages from the Bioconductor project executed in the R programming environment (1). Raw image data were imported into Bioconductor using readIllumina as implemented in the beadarray package (2) with background subtraction and image sharpening. The resulting bead-level data was then normalized for intensity at the bead level using the HULK algorithm (3, 4), to adjust for local spatial effects (i.e. cross-array gradients). The data were then summarized for each bead type. A model-based variance stabilizing transformation, which generates values on a log2 scale for compatibility with downstream analyses(5) was applied to the bead-type summaries, followed by quantile normalization (6) across the experiment using functions in the beadarray package. Bead-types not detected on at least 1 array (detection $p<0.01$) were then filtered to improve power to detect differentially expressed genes (7). We assessed differential expression after 21 days of IL-13 treatment (IL-13 versus control) using linear models and empirical Bayes moderated F statistics as implemented in the LIMMA package (8). We considered differences in gene expression significant if P values were <0.05 after adjustment for multiple testing as described previously (9), so that false discovery rate was <5%. Bead-types were annotated to genes using a combination of the manufacturer's annotation, transcript level annotations obtained from AceView (10), and annotations from the University of Cambridge Computational Biology Group (11) in order to optimize interpretation of the gene expression data(12). We performed visualization and plotting using TIBCO Spotfire DecisionSite for Functional Genomics (TIBCO Spotfire, Somerville, MA, USA). Raw and processed microarray data were deposited in the National Center for Biotechnology Information Gene Expression Omnibus (13) and are accessible through GEO Series accession number GSE37693:
http://www.ncbi.nlm.nih.gov/geo/query/acc.cgi?token=pdixdmkcecigcpk&acc=GSE37693.

Real-time quantitative PCR assay. RNA was purified using the RNeasy kit (Qiagen, Valencia, CA) and reverse transcribed using High-Capacity cDNA Archive kit (Life Technologies, Carlsbad, CA). Target mRNA levels were quantified with real-time PCR using fluorogenic probe/primer combinations specific for the target gene and TaqMan FAST Universal master mix (Life Technologies). Probe/primer sequences are provided in Supplemental Table 5. All PCR assays were quantitative and utilized plasmids containing the target gene sequences as standards. All probes were designed to span an intron and did not react with genomic DNA. Copy numbers of *MAPK13*, *MAPK14*, and mouse *Gapdh* mRNA were determined using pre-designed TaqMan assays (Life Technologies). The cDNAs for *CLCA1, CLCA2, GAPDH,* mouse *Clca3*, mouse *Gapdh*, and portions of *MUC5AC*, *MUC5B*, and mouse *Muc5ac* were amplified by PCR from RNA purified from hTEC or mTEC cultures and reversed transcribed to cDNA. The resulting PCR products were blunt cloned into PCR.Blunt vector (Invitrogen) and used as standards for the determination of the copy numbers of these genes. The plasmids encoding all other target genes were obtained from Thermo Scientific Open Biosystems (Huntsville, AL). Preliminary experiments established consistency of GAPDH levels under the present experimental conditions.

Immunostaining. Mouse anti-human MUC5AC biotin-conjugated mAb clone 45M1 was obtained from Thermo Lab Vision (Kalamazoo, MI). Rabbit anti-human CLCA1 polyclonal Ab (#1228, Open Biosystems, Rockford, IL) was generated by peptide inoculation and peptide-based affinity purification using amino acids 681-693 as described previously (14). For immunocytochemistry, cells were fixed in 0.4% paraformaldehyde, permeabilized in PBS with 1% Tween-20), subjected to heat-induced epitope retrieval in 10 mM sodium citrate buffer (pH 6), blocked with Image-It FX signal enhancer, with 2% fish gelatin (Sigma), and then incubated with anti-MUC5AC biotin-conjugated mAb and rabbit anti-CLCA1 antibody followed by Alexa 488- or 555-conjugated streptavidin or Alexa 555- or 633-conjugated goat anti-rabbit secondary Ab (Life Technologies), counterstained with Sytox Green (Life Technologies) or DAPI (Life Technologies) and then imaged by conventional (Leica) or confocal (Zeiss LSM-510 META or LSM-700 laser scanning confocal microscope) fluorescence microscopy. The LSM-700 microscopy was used to obtain the Z-axis photomicrographs and accompanying video (containing 10 frames that span 3.6 μm of the Z-axis). For immunohistochemistry, lung sections were incubated with citrate-based Antigen Unmasking Solution (Vector Labs, Burlingame, CA) for 10 min at 90 °C for antigen retrieval and then with biotinylated anti-MUC5AC mAb (2 μg/ml) and rabbit anti-CLCA1 Ab (10 μg/ml) in 70 mM NaCl, 30 mM HEPES, 2 mM $CaCl_2$, pH 7.4 with 1% BSA, 1% goat serum, and 0.1% cold water fish gelatin followed by 10 μg/ml Alexa-488 conjugated streptavidin and 10 μg/ml Alexa-555 conjugated goat anti-rabbit IgG (Life Technologies) in the same buffer overnight at 4 °C.

Generation of shRNA-expressing cells. Lentiviral transfection efficiencies were 50-60% as determined using the MISSION Turbo-GFP control vector (SHC003, Sigma), and a representative example is provided in Supplemental Figure 3.

Cell-based MUC5AC ELISA. Cells were fixed with 4% formaldehyde, rinsed with wash buffer (PBS with 0.1% Triton), incubated with blocking buffer containing 1X milk (BioFX Company, Owings Mills, MD) for 1 h at 25 °C, rinsed again, and incubated with mouse anti-human MUC5AC biotin-conjugated mAb clone 45M1 at 1:500 final dilution for 18 h at 4 °C. Cells were then rinsed and incubated with neutravidin-horseradish peroxidase (Pierce Biotechnology, Rockford, IL) at a final dilution of 1:2000 for 1 h at 25 °C followed by developing solution (R&D Systems, Minneapolis, MN). The reaction was terminated using stop solution (R&D Systems) and absorbance measured at 450 nm. Cells were incubated with 0.5% crystal violet solution for 30 min at 25 °C, washed, and incubated with 1% SDS (100 μl/well) for 1 h at 25 °C for absorbance at 595 nm.

Standard-based MUC5AC ELISA. Cells and tissues were lysed in the mammalian protein extraction reagent (M-PER, Thermo Pierce Biotechnology) supplemented with Halt Protease & Phosphatase Inhibitor Cocktail (Thermo Pierce Biotechnology) and 5 mM EDTA. Protein concentration was determined using the BCA protein assay kit (Thermo Pierce Biotechnology). For analysis of MUC5AC levels in the apical supernatants, PBS (0.2 ml) was added to the apical side of hTEC cultures for 15 min at 37 °C before collection of the apical supernatant.

CLCA1 ELISA based on anti-CLCA1 polyclonal Ab. Rabbit anti-human CLCA1 polyclonal Ab (#1228) was generated as described above. To generate the CLCA1 standard, recombinant CLCA1-3xFLAG containing amino acids 681-693 was expressed in 293Tcells using the pCDNA3.1 vector (Life Technologies) and purified using anti-3xFLAG antibody (Sigma). ELISA plates (Thermo Scientific Nagle Nunc) were coated with 50-µl sample aliquots (1 µg/well total protein) or with varying concentrations of standard overnight at 4 °C, washed, blocked with 3% fish gel in PBS for 2 h at 25 °C, washed again, and anti-CLCA1 polyclonal Ab was added at a final dilution of 1:100 for 1 h at 25 °C. The plates were washed, and HRP-conjugated goat anti-rabbit secondary antibody (Santa Cruz) was added at 1:2000 dilution for 1 h at 25 °C. Ab-binding was detected using color developing solutions (R&D Systems) with absorbance at 450 nm on a Spectra Max Plus plate reader (Molecular Devices, Sunnyvale, CA).

CLCA1 ELISA based on anti-CLCA1 mAb. To generate the standard, a plasmid encoding the N-terminal portion of CLCA1 (N-CLCA1, amino acids 22-694) with a 6-His tag was expressed in 293F cells and purified by affinity chromatography. Cell and tissue samples were lysed in M-PER reagent (Thermo Pierce Biotechnology) and lysates (10 µg/well) were plated in carbonate-bicarbonate buffer pH 9.4 overnight at 4 °C. The plates were washed, blocked overnight with Sea Block blocking buffer (Thermo Pierce Biotechnology), washed again, and anti-CLCA1 8D3 mAb was added at 1 µg/ml for 3 h. The plates were washed and HRP-conjugated Fab fragment of goat anti mouse IgG (H+L chains) antibody (Life Technologies) at 1:2000 was added for 1 h. After washing, Ab binding was detected using the 1-Step Ultra TMB-ELISA substrate (Thermo Pierce Biotechnology) with absorbance at 450 nm on the Spectra Max Plus plate reader. For analysis of CLCA1 leves in the apical supernatants, the apical supernatant was collected as described above.

Generation of anti-CLCA1 mAb. To generate immunogen, N-CLCA1 was purified from baculovirus-infected insect cells (Hi5) in a customized pFastBac Dual vector in frame with an N-terminal honey bee mellitin signal sequence and C-terminal thrombin cleavage site followed by a 6-His tag. Recombinant baculovirus was generated in Sf9 insect cells. Recombinant N-CLCA1 was produced by infecting Hi5 cells cultured in serum-free ExCell 405 media. Culture supernatants were collected 72 hours post-infection and the proteins were purified to homogeneity using Ni-affinity chromatography followed by ion-exchange chromatography. Protein identity was verified by Western blot against the 6-His tag and purity was assessed by Coumassie-stained SDS-PAGE. For generation of mAbs, BALB/cJ mice were primed and boosted at 3-wk intervals with purified N-CLCA1 (50 µg) complexed with adjuvant. Approximately one month after the last boost, serum was harvested and tested for immunoreactivity against plate-immobilized N-CLCA1 purified from 293T cells. Mice with highest titers were boosted intravenously with N-CLCA1 (50 µg) and splenocytes were harvested 3 days later. Hybridomas were produced by fusion with P3X63Ag8.653 myeloma cells. Screening for positive clones was performed with ELISA using the pure insect-cell-generated N-CLCA1. Protein A/G chromatography was used to purify the mAbs. To screen hybridomas for anti-CLCA1 mAb production, ELISA plates (Thermo Scientific Nagle Nunc) were coated with recombinant purified N-CLCA1 overnight at 4 °C, washed twice with 0.1% Triton in PBS, and then blocked with 3% fish gel in PBS for 2 h at 25 °C. The plates were washed twice and hybridoma supernatants were added. The plates were washed, and HRP-conjugated goat anti-rabbit secondary antibody (Santa Cruz) was added at 1:2000 dilution for 1 h at 25 °C. Plates were washed, and Ab-binding was detected using color developing solutions (R&D Systems) for absorbance at 450 nm on a Spectra Max Plus plate reader (Molecular Devices, Sunnyvale, CA).

Gene knockdown with siRNA. For transfection, lipofectamine (2.5 µl) was mixed in RPMI-serum free media (200 µl) with RNAi (25 nM) by shaking for 30 min at 25 °C. Transfection efficiency was determined using Block-it fluorescent oligo (Life Technologies) at 24 h after transfection and ranged from 60-65%.

Mouse experiments in cultured cells and whole animals. *Mapk13*$^{-/-}$ mice (15) were obtained from Ana Cuenda (Universidad de Extremadura, Caceres, Spain), and same-strain C57BL/6J mice were obtained from Jackson Laboratories (Bar Harbor, ME). Mice were treated at 6-9 wk of age with recombinant mouse IL-13 (5 μg) or BSA control in PBS vehicle administered intranasally (on d 0, d 1, and d 2) under sedation with ketamine/xylazine, and lungs harvested (on d 7) for analysis of mRNA level and histology as described previously (16-18). Mouse tracheal epithelial cell (mTEC) cultures were isolated and maintained under air-liquid interface (ALI) conditions as described previously (19). For the present experiments,

mTEC cultures were seeded at $2x10^5$ cells/cm^2 on d 0, switched to air-liquid interface conditions on d 7, and then incubated with or without mouse IL-13 (Peprotech, Rocky Hill, NJ) at 10 ng/ml on d 14-21 for analysis at that time.

MAPK13 inhibitor assay. Full-length 6-His-tagged MAPK13 and constitutively active GST-MKK6 were prepared as described below. Activated MAPK13 was generated in 50 mM Hepes, 10 mM $MgCl_2$ and 1 mM DTT, containing 1 μM MAPK13, 2 μM MKK6 and 50 μM ATP for 1 h at 25 °C. MKK6 was removed by incubation with glutathione Sepharose 4B beads (GE Healthcare Biosciences). MAPK13 activation was confirmed by Western blot using anti-phospho-p38-MAPK (T180/Y182) antibody (R&D Systems, Minneapolis, MN). IMAP assays were performed in 96-well non-treated half-area black plates or 384-well black plates (Corning Inc., Corning, NY) in a final reaction volume of 20 μl using the linear phase of the rate kinetics. The peptide substrate was a kind gift from J. Schindler (Washington University). Assay reactions proceeded for 20 min at 25 °C in 10 mM Tris-HCl, 10 mM $MgCl_2$, 0.1% BSA, 0.05% NaN_3, 1 mM DTT, pH 7.2 after which 60 μl of tri-valent metal nanoparticles containing IMAP binding reagent (Molecular Devices, Sunnyvale, CA) was added for 80 min at 25 °C. The IMAP binding reagent was optimized at 1:600 (vol/vol) based on the number of acidic residues in the peptide substrate. Fluorescence polarization was measured with a Biotek Synergy 4 multimode plate reader (Biotek, Winooski, VT) with excitation at 485 nm and emission at 528 nm. Curve fitting was performed using GraphPad Prism software (Graphpad Software, La Jolla, CA).

MAPK14 inhibitor assay. MAPK14 kinase activity was measured similar to that of MAPK13 with a few exceptions. Full-length GST tagged MAPK14 was purified as described below. To activate MAPK14, 5 μg MKK6 (S207D/T211D) (Abnova, Taipei, Taiwan) was added to a 1 ml reaction containing 1μM MAPK14. The reaction was carried out at room temperature, whereafter MAPK14 phosphorylation was validated by western blot using anti-phospho-p38 antibody. After a freeze-thaw cycle, MAPK14 kinase activity was tested and EC_{80} was estimated to be 70nM. Inhibitors were analyzed for the potency against MAPK14 as described above for MAPK13 except that the kinase reaction was carried out for 80 min before addition of tri-valent metal nanoparticles.

MAPK purification for biochemical assays and crystallization. Full-length human MAPK13 (1-365), MAPK14 (1-360), and MAPK13 crystallization construct (1-352) were cloned into pET28a as N-terminal 6-His-tagged constructs. A constitutively active mutant MKK6-GST fusion construct (GST-MKK6 Glu) was a kind gift from Peiqing Sun (Scripps, La Jolla, CA). A pET28a construct of λ-phosphatase was a kind gift from Dima Klenchin (University of Wisconsin, Madison, WI). All constructs were confirmed by sequencing and transformed into Rosetta2 (DE3) *E. coli* (EMD Millipore, Billerica, MA) and expressed as soluble proteins that were purified using the specific affinity tags followed by gel filtration chromatography. The MAPK13 proteins expressed in *E. coli* displayed a high degree of auto-phosphorylation, so they were dephosphorylated with λ-phosphatase prior to final purification by ion exchange (Mono Q). All buffers used during purification (lysis, column, and storage) of MAPKs required addition of 10% glycerol and 1-5 mM reducing agent (either β-mercaptoethanol or DTT) to prevent precipitation of the recombinant protein. The final purified MAPK13 for crystallization was stored in buffer containing 20 mM Hepes pH 7.5, 150 mM NaCl, 10% glycerol, and 1 mM DTT.

Supplemental References

1. Gentleman, R.C., Carey, V.J., Bates, D.M., Bolstad, B., Dettling, M., Dudoit, S., Ellis, B., Gautier, L., Ge, Y., Gentry, J., et al. 2004. Bioconductor: open software development for computational biology and bioinformatics. Genome Biol. 5:R80.

2. Dunning, M.J., Smith, M.L., Ritchie, M.E., and Tavare, S. 2007. beadarray: R classes and methods for Illumina bead-based data. Bioinformatics 23:2183-2184.

3. Cairns, J.M., Dunning, M.J., Ritchie, M.E., Russell, R.C., and Van den Hurk, A.F. 2008. BASH: a tool for managing BeadArray spatial artefacts. Bioinformatics 24:2921-2922.

4. Lynch, A.G., Dunning, M.J., Iddawela, M., Barbosa-Morais, N.L., and Ritchie, M.E. 2009. Considerations for the processing and analysis of GoldenGate-based two-colour Illumina platforms. Stat. Methods Med. Res. 18:437-452.

5. Lin, S.M., Du, P., Huber, W., and Kibbe, W.A. 2008. Model-based variance-stabilizing transformation for Illumina microarray data. Nucleic Acids Res 36:e11.

6. Bolstad, B., Irizarry, R., Astrand, M., and Speed, T. 2003. A comparison of normalization methods for high density oligonucleotide array data based on variance and bias. Bioinformatics 19:185-193.

7. Hackstadt, A.J., and Hess, A.M. 2009. Filtering for increased power for microarray data analysis. BMC Bioinformatics 10:11.

8. Smyth, G.K. 2004. Linear models and empirical Bayes methods for assessing differential expression in microarray experiments. In Stat. Appl. Genet. Mol. Biol.

9. Benjamini, Y., and Hochberg, Y. 1995. Controlling the false discovery rate — a practical and powerful approach to multiple testing. J. R. Stat. Soc. B 57:289-300.

10. Thierry-Mieg, D., and Thierry-Mieg, J. 2006. AceView: a comprehensive cDNA-supported gene and transcripts annotation. Genome Biol 7 Suppl 1:S12 11-14.

11. Barbosa-Morais, N.L., Dunning, M.J., Samarajiwa, S.A., Darot, J.F., Ritchie, M.E., Lynch, A.G., and Tavare, S. 2010. A re-annotation pipeline for Illumina BeadArrays: improving the interpretation of gene expression data. Nucleic Acids Res 38:e17.

12. Yin, J., McLoughlin, S., Jeffery, I.B., Glaviano, A., Kennedy, B., and Higgins, D.G. 2010. Integrating multiple genome annotation databases improves the interpretation of microarray gene expression data. BMC genomics 11:50.

13. Edgar, R., Domrachev, M., and Lash, A.E. 2002. Gene Expression Omnibus: NCBI gene expression and hybridization array data repository. Nucl. Acids Res. 30:207-210.

14. Gibson, A., Lewis, A.P., Affleck, K., Aitken, A.J., Meldrum, E., and Thompson, N. 2005. hCLCA1 and mCLCA3 are secreted non-integral membrane proteins and therefore are not ion channels. J. Biol. Chem. 280:27205-27212.

15. Sabio, G., Simon, J., Arthur, C., Kuma, Y., Peggie, M., Carr, J., Murray-Tait, V., Centeno, F., Goedert, M., Morrice, N.A., et al. 2005. p38g regulates the localisation of SAP97 in the cytoskeleton by modulating its interaction with GKAP. EMBO J. 24:1134-1145.

16. Tachdjian, R., Mathias, C., Khatib, S.A., Bryce, P.J., Kim, H.S., Blaeser, F., O'Connor, B.D., Rzymkiewicz, D., Chen, A., Holtzman, M.J., et al. 2009. Pathogenicity of a disease-associated human IL-4 receptor allele in experimental asthma. J. Exp. Med. 206:2191-2204.

17. Patel, A.C., Morton, J.D., Kim, E.Y., Alevy, Y., Swanson, S., Tucker, J., Huang, G., Agapov, E., Phillips, T.E., Fuentes, M.E., et al. 2006. Genetic segregation of airway disease traits despite redundancy of chloride channel calcium-activated (CLCA) family members. Physiol. Genomics 25:502-513.

18. Kim, E.Y., Battaile, J.T., Patel, A.C., You, Y., Agapov, E., Grayson, M.H., Benoit, L.A., Byers, D.E., Alevy, Y., Tucker, J., et al. 2008. Persistent activation of an innate immune response translates respiratory viral infection into chronic inflammatory lung disease. Nat. Med. 14:633-640.

19. You, Y., Richer, E.J., Huang, T., and Brody, S.L. 2002. Growth and differentiation of mouse tracheal epithelial cells: selection of a proliferative population. Am. J. Physiol. Lung Cell Mol. Physiol. 283:L1315-1321.

Supplemental Table 1. Clinical characteristics of lung transplant donors without COPD (Non-COPD) and recipients with very severe (GOLD Stage IV) COPD (COPD). Only limited data is available for lung transplant donors.

Characteristic	Non-COPD	COPD
Number per group	11	20
Mean age (range)	38 (11-56)	59 (47-68)
Male: Female	7:4	9:11
FVC (L)	–	1.97 ± 0.63*
FVC (% predicted)	–	52.9 ± 14.7*
FEV_1 (L)	–	0.55 ± 0.17*
FEV_1 (% predicted)	–	19.0 ± 4.35*
FEV_1/FVC	–	0.29 ± 0.08*
DLCO		5.64 ± 2.66*
DLCO (% predicted)		25.3 ± 6.78*
Pack years (range)	0-20	25-95

*Values represent mean ± SD.

Supplemental Table 2. Data collection and refinement statistics for MAPK13 complexes with inhibitor compounds.

Compound	None	61	124
Data collection statistics			
Space group	$P2_12_12_1$	$P2_12_12_1$	$P2_12_12_1$
Cell dimensions			
a, *b*, *c* (Å)	60.9, 69.4, 92.5	60.9, 69.9, 92.8	61.1, 69.6, 93.2
α, β, γ (°)	90, 90, 90	90, 90, 90	90, 90, 90
Resolution (Å)	50.0-1.70(1.76-)*	50.0-2.10(2.18-)	50.0-2.35(2.43-)
R_{sym} or R_{merge}	0.065(0.504)	0.068(0.360)	0.070(0.253)
$I / \sigma I$	29.6(4.1)	25.9(4.7)	23.8(5.5)
Completeness (%)	99.3(99.7)	90.4(98.9)	93.6(99.9)
Redundancy	6.7(6.9)	6.4(6.0)	5.4(5.7)
Refinement statistics			
Resolution (Å)	35.0-1.70	35.0-2.10	35.0-2.35
No. reflections	43514	21034	15873
R_{work} / R_{free}	0.201/0.220	0.242/0.275	0.203/0.269
No. atoms			
Protein	2781	2753	2753
Ligand/ion	0	27	28
Water	319	277	111
B-factors			
Protein	32.4	37.1	37.1
Ligand/ion	N.A.	26.9	29.0
Water	42.3	40.6	37.7
R.m.s. deviations			
Bond lengths (Å)	0.003	0.004	0.004
Bond angles (°)	0.739	0.844	0.815

*Values in parentheses are for highest-resolution shell.

Supplemental Table 3. Values for IC_{50} for inhibition of MAPK13 activity.

Compound	IC_{50} (nM)[1]	95% Confidence	R^2
62	281	209.8-374.9	0.98
61	620	530.1-723.9	0.99
43 (BIRB-796)	1968	1547-2503	0.99
47 (AMG-548)	7736	6467-9253	0.99
124	98747	28862-337855	0.9
104 (SB203580)	NC	–	0.90
DMSO (vehicle)	NC	–	0.30

[1]MAPK13 IC_{50} determined using IMAP-based biochemical assay. NC: data not converged to model due to compound inactivity.

Supplemental Table 4. Values for IC_{50} for inhibition of MAPK14 activity.

Compound	IC_{50} (nM)[1]	95% Confidence	R^2
62	0.04	8.54e-006-181.6	0.67
61	3.60	1.74-7.46	0.94
43 (BIRB-796)	0.10	0.003-2.51	0.51
47 (AMG-548)	0.03	0.02-0.06	0.78
124	12838	4436-37153	0.94
104 (SB203580)	6.26	2.98-1314	0.90
DMSO (vehicle)	NC	–	–

[1]MAPK14 IC_{50} determined using IMAP-based biochemical assay. NC: data not converged to model due to compound inactivity.

Supplemental Table 5. Probe and primer sequences for real-time quantitative PCR assays of human and mouse target genes.

Gene	Forward Oligo	Reverse Oligo	Probe
Human:			
GAPDH	CAGCCGAGCCACATCCCTCAGACACCAT	CTTTACCAGAGTTAAAAGCAGCCCTGGTGACCA	AGGTCGGAGTCAACCGATTTGGTCGTATTG
MUC5AC	AGGCCAGCTACCGGGCCGGCCAGACCAT	GTCCCCGTACACGGCGCAGGTGGCCAGGCA	TGCAACACCTGCACCTGTGACAGCAGGAT
CLCA1	AGTGTCACAGCCCTGATTGAATCAGTGAAT	AGTTGTGAAATACCTTGAGTAGACACCGT	TAATGGAGCAGGTGCTGATGCTACTAA
CLCA2	ACCCTATCTTGGACAGCACCTGGAGAA	CTTGGATATTCTGTAGACTTTTACTCA	TTTGATCAGGGCCAGGCTA-CAAGCTATGAA
CLCA4	TGGACATACAGAAGTTTTGGAACT	GCTGTAAAATACCTGGAGTAGACT	GATAATGGTGCAGGCGCTGATTCTTTCAAGAA
MAPK13	Life Technologies Hs00559623		
MAPK14	Life Technologies Hs00176247		
MUC5B	GTGCCTCCGGAGCTGCCACACGCTGGA	ACTCCCATCCGACACCAGCCCCGG	GGGCTGTTTCAGCACACACTGCGTGTCCGGCCT
Mouse			
GAPDH	Life Technologies #4308313		
MUC5AC	TACCACTCCCTGCTTCTGCAGCGTGTCA	ATAGTAACAGTGGCCATCAAGGTCTGTCT	TATACCCCTTGGGATCCATCATCTACA
MAPK13	GATCATGGGGATGGAATTCA	ATGCCAGCGGAGTGGATGTA	GGTCCAGTACTTGGTGTACC
MAPK14	GGAACCCCAGGGGCTGAGCTT	GTTCATCTTCGGCATCTGGGCCA	ATCTCCTCAGAGTCTGCAAGA
CLCA3	ACCGGCTGCCGCTAAAGAGCTTGAG	AGACCATTGTTCTGAACCTGATCCGAAG	AGCTGTCCAAAATGACAGGAGGCCTGCAGACATA
CLCA4	ACAGTAAGAAAGCCAGAAATCA	CGAAGGCGAACAGAGAAGATATTTAGCT	TACACCACCTCCGATTTCCAGGAAGAT
CLCA5	CTGGCCTTTCGGACAGCCAGCCTTAAGA	AATGGTGGGTGTTGTTCAGCGTGTAAGT	AGTGCCCATGCTTAGCTGTCCCTG
CLCA6	TGCCAATGGAGAAGCACTT	ATTCGAATTCAGGCGATCATA	TGGAGAGGGTGACGTCTCCAT
CLCA7	TGCCAATGGAGAAGCACTT	ATTCTATTCAGACGGTCAGA	ATGGAGACACCACCGGCTCCA

Supplemental Figure 1

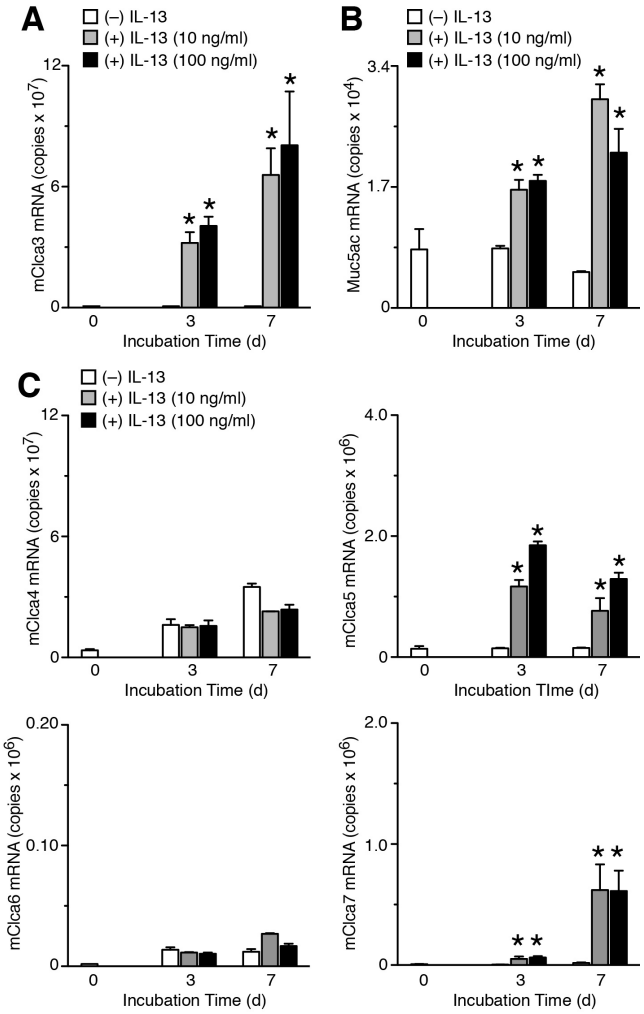

Supplemental Fig. 1. IL-13-stimulated *Clca* and *Muc5ac* gene expression in mouse airway epithelial cells. (**A**) Levels of mClca3 mRNA in primary-culture mouse tracheal epithelial cells (mTECs) cultured under air-liquid interface conditions and incubated with or without IL-13 for the indicated times and then analyzed using real-time quantitative PCR assay. (**B**) For conditions in (A), corresponding values for *Muc5Ac* mRNA. (**C**) For conditions in (A), corresponding values for mClca4, mClca5, mClca6, and mClca7 mRNA. Values represent mean ± SEM (n = 3 experiments).

Supplemental Figure 2

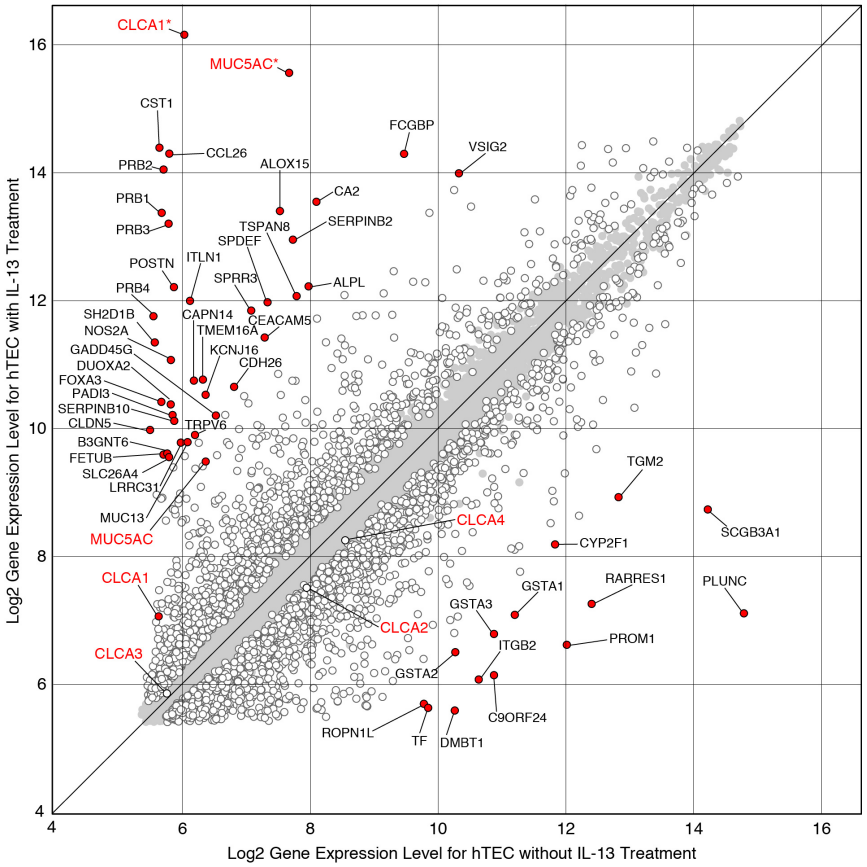

Supplemental Fig. 2. IL-13-driven gene expression in human airway epithelial cells. Oligonucleotide microarray analysis of mRNA from primary-culture human airway epithelial cells (hTECs) treated with versus without IL-13 (50 ng/ml for 21 days). Scatter plot depicts log 2 normalized gene expression. Each symbol represents the expression value for an individual gene with differentially expressed genes colored red or white, and genes not differentially expressed colored gray. Genes colored red indicate top 50 differentially expressed genes based on absolute fold-change, along with *MUC5AC* (array rank 74) and *CLCA1* (array rank 427). Values represent results from quadruplicate microarray chips for each experimental condition. * indicates corresponding values for *MUC5AC* and *CLCA1* expression derived from real-time quantitative PCR assay for comparison to microarray values.

Supplemental Figure 3

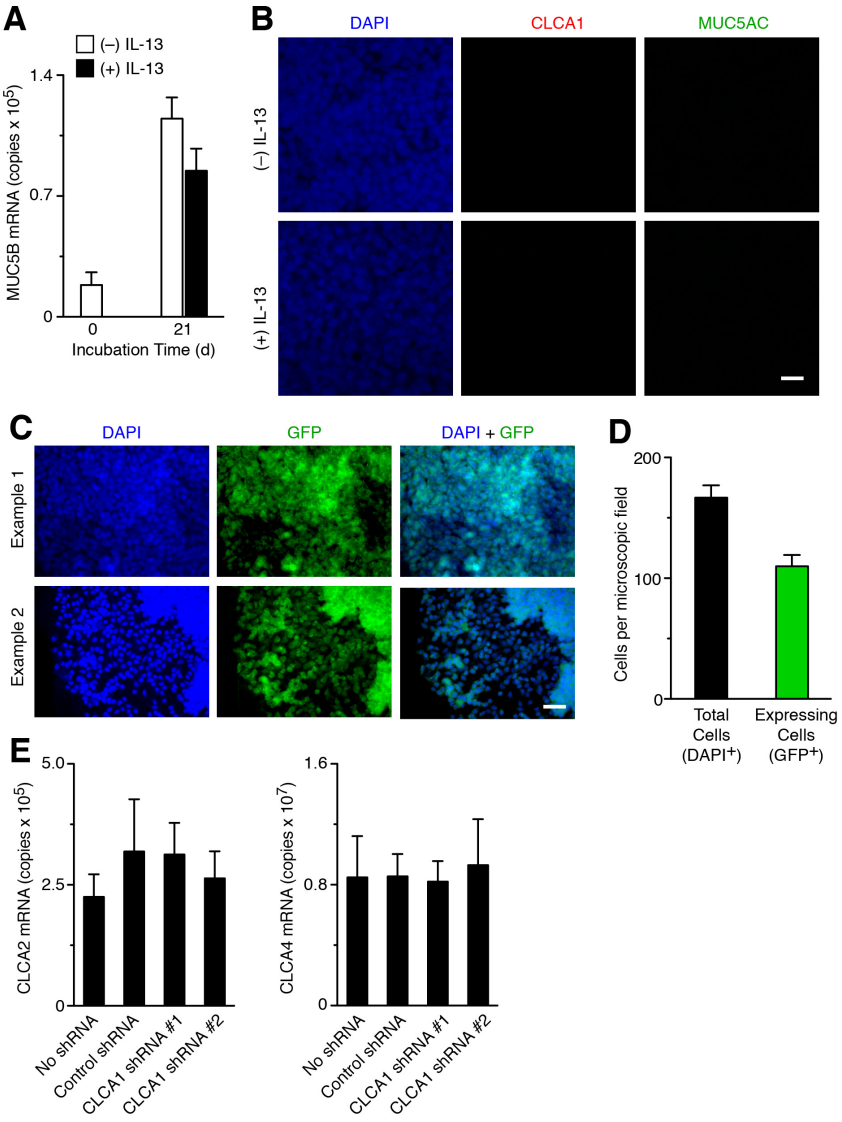

Supplemental Fig 3. Characteristics of human airway epithelial cell cultures. (**A**) Levels of *MUC5B* mRNA levels by real-time quantitative PCR (qPCR) assay as a control for Fig. 1A. All values represent mean ± SEM. (**B**) Representative photomicrographs for DAPI staining and CLCA1 and MUC5AC immunostaining in the absence of primary antibody using primary-culture hTECs with and without incubation with IL-13 (50 ng/ml) as a control for Fig. 1E. Bar = 50 µm. (**C**) Representative photomicrographs of hTEC cultures transfected with Turbo-GFP at MOI 1 for 24 h. Bar = 50 µm. (**D**) Corresponding quantification of transfection efficiencies for conditions in (C). (**E**) Levels of CLCA2 and CLCA4 mRNA in hTECs that were transduced with lentivirus encoding CLCA1 or control shRNA as a control for Fig. 1G.

Supplemental Figure 4

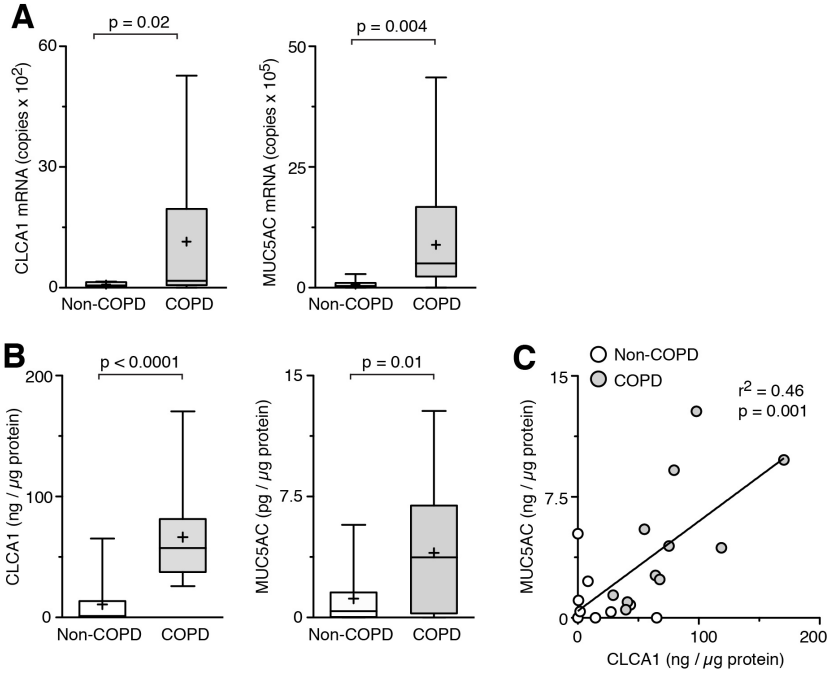

Supplemental Fig 4. Analysis of gene expression in airway-containing cores from lung tissues from non-COPD and very severe COPD subjects. (**A**) Levels of *CLCA1 and MUC5AC* mRNA in lung tissue samples containing airways from non-COPD (n = 17 airway cores from 7 subjects) and very severe COPD (n =17 cores from 11 subjects). (**B**) Levels of CLCA1 and MUC5AC protein in lung tissue lysates from non-COPD (n=9) and COPD (n=11) subjects. (**C**) For data in (B), Pearson correlations of CLCA1 and MUC5AC protein levels in non-COPD and COPD subjects (n=20 total subjects).

Supplemental Figure 5

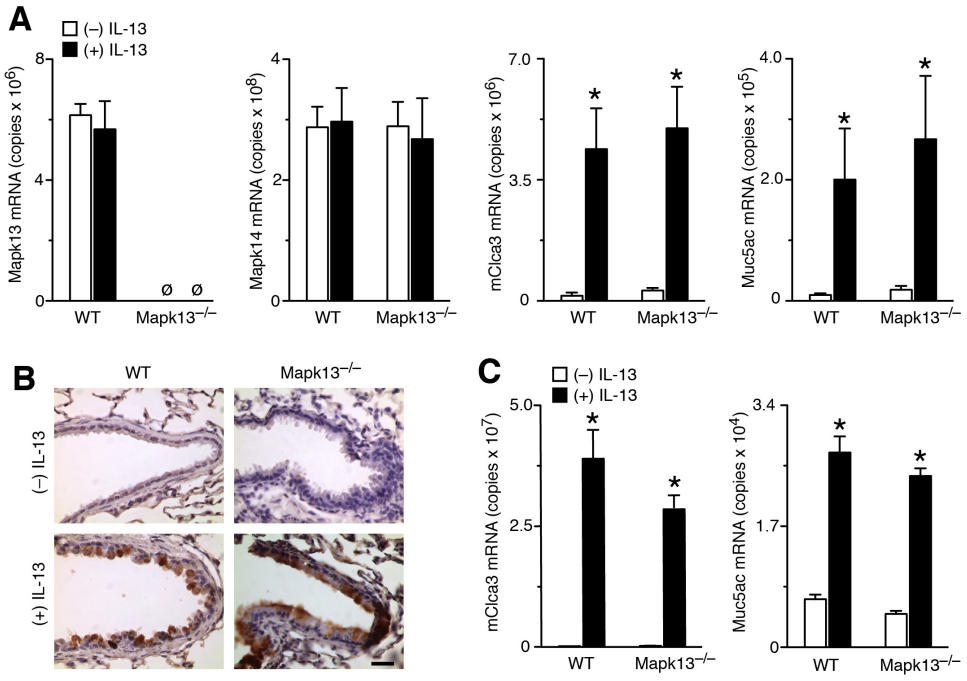

Supplemental Figure 5. Effect of Mapk13 deficiency on IL-13-induction of *mClca3* and *Muc5ac* gene expression in mice in vivo and in vitro. (**A**) Levels of *Mapk13*, *Mapk14*, *mClca3*, and *Muc5ac* mRNA in lungs from *Mapk13*$^{-/-}$ and same-strain wild-type control mice with and without IL-13 treatment administered intranasally for 3 d and assessed at 7 d. (**B**) For conditions in (A), representative photomicrographs of lung sections immunostained for Muc5ac. Bar = 100 µm. (**C**) Levels of *mClca3* and *Muc5ac* mRNA in primary-culture mouse tracheal epithelial cells (mTECs) incubated with and without IL-13 (10 ng/ml) for 7 d. For (A,C), all values represent mean ± SEM, and * indicates a significant difference from corresponding control value for no IL-13 treatment.

Supplemental Figure 6

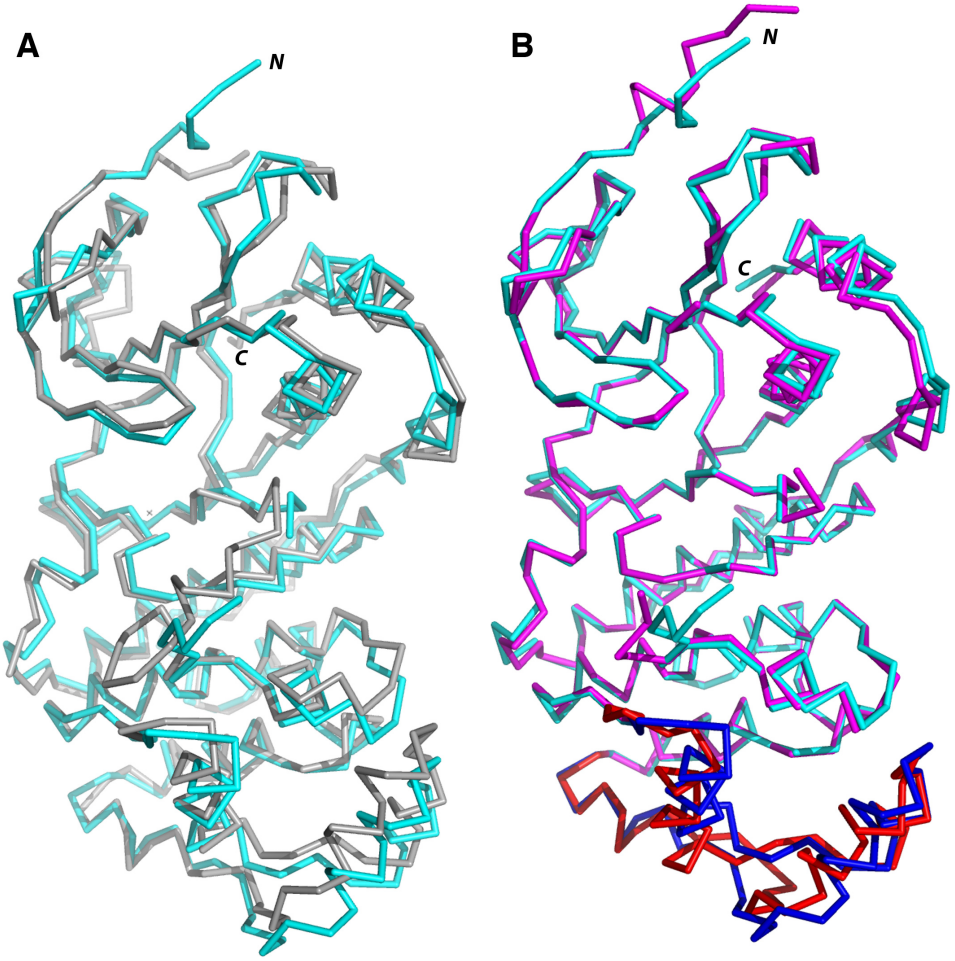

Supplemental Fig 6. (**A**) Superposition of MAPK13 inactivated apo structure (cyan) with MAPK14 (gray; PDB ID: 1RC3). MAPK13 displays 60% sequence identity with MAPK14. Correspondingly, the structures overlap very closely with 1.8 Å RMSD (for 332 C-alphas). (**B**) Comparison of MAPK13 apo structure determined here (cyan) with a previously deposited MAPK13 structure at lower resolution (magenta; 3COI). Overall, the structures are very similar (1.6 RMSD for 351 C-alphas), except in the region of 223 – 272 (highlighted in blue for the present analysis and red for 3COI), where the structures diverge considerably (2.6 Å RMSD for those residues). The two proteins crystallize in nearly identical unit cells, thus this does not appear to be an artifact of crystal packing.

Supplemental Figure 7

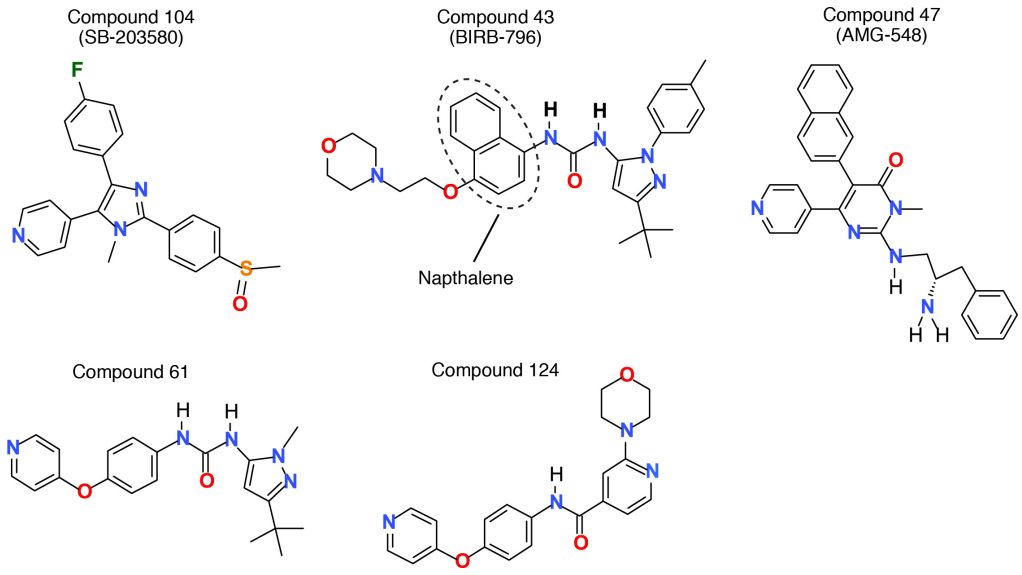

Supplemental Fig. 7. Chemical structures of representative inhibitors for MAPK13 and MAPK14. The naphthalene moiety is highlighted in the structure for BIRB-796.

Supplemental Figure 8

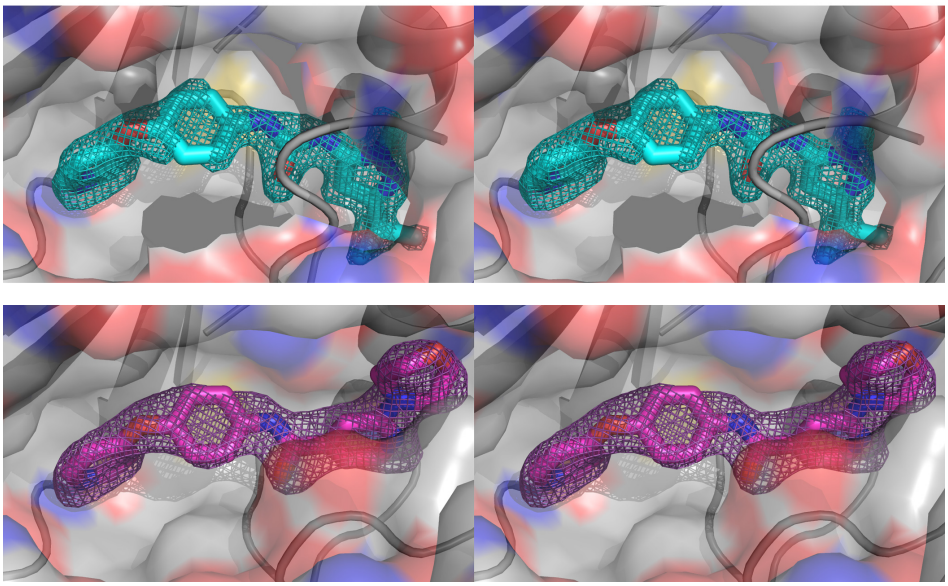

Supplemental Fig 8. Side-by-side stereo view of compound 61 (cyan) and compound 124 (magenta) co-crystal structures with MAPK13. Difference electron density (Fo-Fc at 3.0σ) for the compounds following initial rigid-body refinement of MAPK13 is shown in mesh.

Supplemental Figure 9

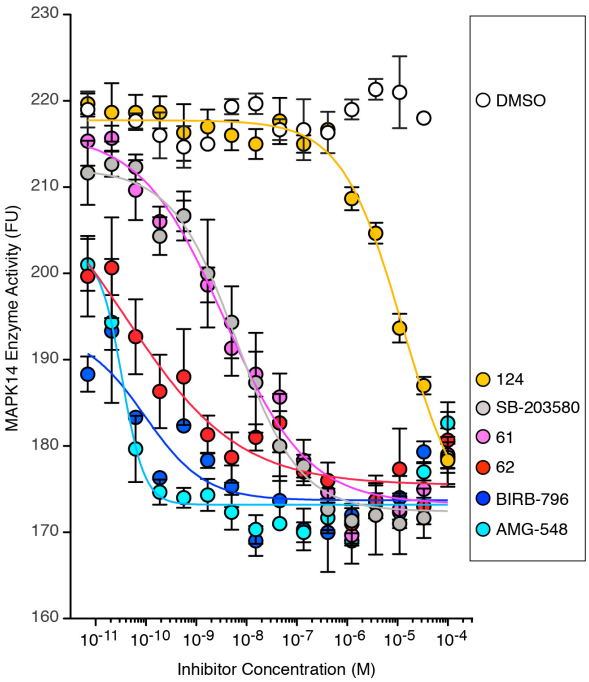

Supplemental Fig 9. Effect of inhibitors on MAPK14 activity. Full (16-point) concentration-response for MAPK14 inhibition for indicated test compounds. Values represent fluorescence polarization (mP) from IMAP assay.

Supplemental Figure 10

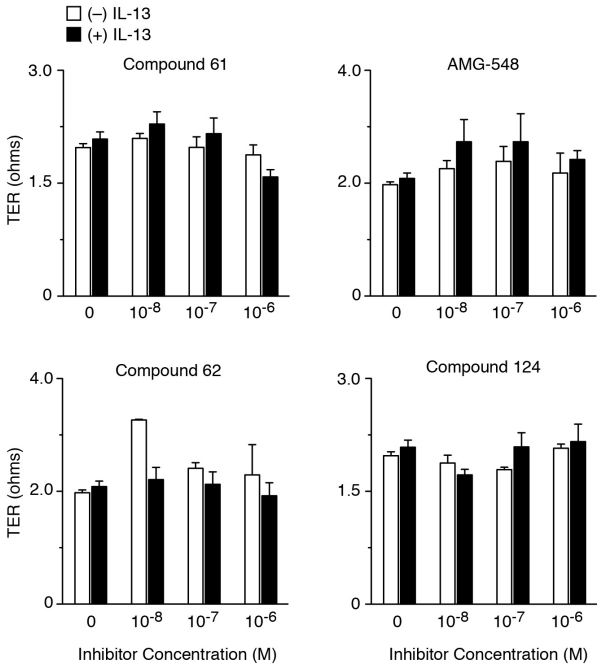

Supplemental Fig 10. Effect of representative compounds on transepithelial electrical resistance (TEER).) hTECs were cultured with or without IL-13 for 21 days with the indicated compounds, and levels of TEER were determined as an index of cellular integrity. Values represent mean ± SEM

Supplemental Video 1. Z-axis as depicted by a Z-stack of representative photomicrographs from confocal microscopy of primary-culture hTECs treated with IL-13 and then immunostained for CLCA1 and MUC5AC and counterstained with DAPI. Z-stack dimensions = 160 μM × 160 μM × 3.6 μM. Red = CLCA1, Green = MUC5AC, and Blue = DAPI.